Fullerene Dimers: Cohesive Energy, Electronic Structure, and Vibrational Modes

Mark R. Pederson
Complex Systems Theory Branch, Naval Research Laboratory, Washington, D.C. 20375

Andrew A. Quong
Sandia Livermore National Laboratory, Livermore, California 94551-0969
(Received 4 May 1994)

To address experiments suggesting the polymerization of C_{60}, via four-membered rings, we have performed density-functional-based calculations on a $[C_{60}]_2$ dimer. The dimer is bound with respect to the isolated molecules, has a short center-to-center separation, and vibrational signature that is similar to what is observed experimentally.

PACS numbers: 71.25.Pi, 61.46.+w, 71.25.Tn

The x-ray data [1] on RbC_{60} that suggest the C_{60} molecules polymerize along the (110) axis is supported by the appearance of additional IR activity in RbC_{60} and CsC_{60} [2]. As shown in Fig. 1, the polymerization is expected to occur by breaking double bonds on the north and south poles of neighboring molecules and then joining the two molecules by a four-membered ring. Examples of such structures include cubane and cyclobutane, and our calculations, within the local-density approximation (LDA), show that two C_2H_4 molecules can be bound by a four-membered ring (e.g., cyclobutane) with a binding energy of 1.71 eV. The ground-state geometry, exhibited in Fig. 1(a), is composed of a perfect square of carbon atoms with C-C distances of 1.548 Å. We find an activation barrier (of 0.59 eV within LDA) when negatively charged and uncharged C_2H_4 molecules follow a simple path to the dimerized cyclobutane structure [3]. Ecklund and co-workers and Pekker *et al.* suggest polymerization of fullerenes also occurs via the [2 + 2] cycloaddition reaction after an electron is accepted [4,5].

Conventional bonding arguments suggest that polymeric C_{60} chains are energetically unfavorable if the carbon bonds on an isolated ball are thought of as resonating graphite bonds. However, the opposite conclusion follows if the C_{60} molecule is viewed as a collection of single and double bonds. Since the intramolecular C_{60} C-C bond lengths are intermediate between resonating and single or double bond pictures, the *qualitative* stability of C_{60} dimers must be worked out from *quantitatively accurate* calculations. To address the energetic stability of a C_{60} dimer we have tied off the white carbon atoms in Fig. 1 by hydrogen atoms, allowed the resulting $C_{12}H_4$ cluster to relax [6], and then transferred the relaxed structure back to the 120-atom dimer. The connectivity of the two fullerenes is the same as that suggested in Ref. [1(b)]. By performing a complete all-electron, full potential self-consistent LDA calculation on the 120-atom dimer [6], we obtain the Hellmann-Feynman (HF) forces which show that the dimer is indeed close to the local equilibrium geometry with a root-mean-square force of 0.015 hartree/bohr. Compared to two isolated C_{60} molecules in their exact equilibrium geometry ($F_{\rm rms} = 0.0006$ hartree/bohr), the partially annealed C_{60} dimer is more stable by at least 0.2 eV. Further stabilization of the dimer will result as it anneals. Within an averaged quadratic approximation, the relaxation energy depends on $F_{\rm rms}$ and a characteristic diagonal force-constant (FC) matrix element ($h_{\rm avg}$) according to $60|\mathbf{F}_{\rm rms}|^2/2h_{\rm avg}$ per ball. Depending on how the phonon frequencies are averaged, one obtains values of $h_{\rm avg}$ between 0.19 and 0.45 a.u. [7]. This suggests additional stabilization in the range of 0.8 to 2.0 eV. While the important qualitative point is that the dimer is stable by *at least* 0.2 eV, this analysis suggests that the dimer is bound by approximately 1.0 – 2.2 eV. The latter energy range is in accord with the LDA binding energy of the $[C_2H_4]_2$ four-membered ring and with the Arrhenius-type behavior (1.25 eV per ring) observed by Ecklund and co-workers [4(b)] for thermal decomposition of C_{60} oligomers. Previous experience with our basis sets has shown that basis superposition error is small compared to 0.2 eV.

In Fig. 1(b), the C-C bonds that bridge the intermolecular and intramolecular bond lengths are 1.60 and

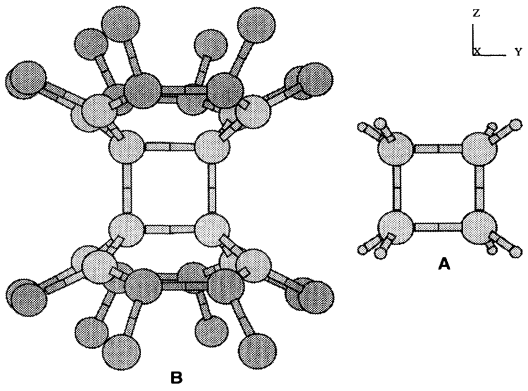

FIG. 1. Connectivity proposed in Ref. [1(b)] and used for our $[C_{60}]_2$ dimer calculations and for the $[C_2H_4]_2$ dimer which exhibits the same bonding characteristics.

 © 1995 The American Physical Society

1.57 Å, respectively. With respect to each molecular center, the four-membered ring dimers are displaced outward by 0.13 Å and the next plane of four atoms relax in the same direction by 0.09 Å. Upon additional relaxation, the action of the forces will cause a slight contraction of the ring bonds and an elongation of the polar region. However, the net force on each of the molecular centers (0.002 hartree/bohr) is essentially zero suggesting that our calculated center-to-center (CTC) distance of 8.81 Å is in accord with the x-ray value of 9.12 Å in the infinite Rb-doped chain [1]. For the $[C_{60}]_2$ dimer and the $[C_2H_4]_2$ dimer, we find intramolecular σ bonds to be 1.57 and 1.55 Å, respectively, suggesting that bond lengths associated with four-membered rings are not strongly dependent on third-neighbor interactions. The addition of an electron to the $[C_2H_4]_2$ dimer perturbs the bond lengths of this molecule by less than 0.5%.

Pictured in Fig. 2 is the electronic density of states (DOS) associated with a dimerized $[C_{60}]_2$. The electronic DOS confirms universal expectations about the electronic and vibrational energy levels. The point-group symmetry of a pair, triplet, n-tuplet, or chain of polymerized C_{60} molecules consists of all reflections (R_8 point-group symmetry). The highly degenerate spectrum of the C_{60} molecule splits into eight different onefold representations that transform like s, x, y, z, xy, yz, zx, and xyz. However, the perturbations along the x and y axes are reasonably mild which causes some of the degeneracies that persisted in the icosahedral molecule to reappear as accidental degeneracies for polymerized balls [e.g., the (x, y) members of the T_{1u} representation and (yz, xz) members of the H_g representation]. Specifically, due to the fact that the lowest unoccupied molecular orbital (LUMO) T_{1u} does not mix heavily with close neighboring (H_u and T_{1g}) representations two distinct T_{1u} peaks appear for the dimer which correspond to the nearly degenerate (x, y) states and the z states, respectively. Perturbations of the energy spectrum are larger in cases where the polymerization couples two representationally distinct but nearly degenerate electronic states. Thus, dimerization causes intramolecular mixing between the nearly degenerate H_g and G_g modes leading to a broadening which is further enhanced by intramolecular coupling between the H_g, G_g, and H_u levels on different balls.

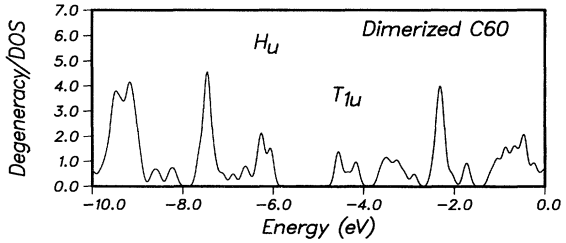

FIG. 2. The electronic DOS of the C_{60} dimer. The LUMO T_{1u} states split into a quasidoublet and singlet state but the HOMO H_u state mixes strongly with the lower G_g and H_g levels leading to a generally broader spectrum.

Mihaly *et al.* [2] have measured the infrared (IR) spectrum associated with C_{60} dimers and polymers. The splittings of the $F_{1u}(3)$ and $F_{1u}(4)$ modes are clear indications of reduced symmetry that occurs in these systems. If one assumes T_h symmetry for the cubic A_1C_{60} crystals the emergence of two IR active peaks, separated by 15 cm^{-1}, in the $F_{1u}(4)$ energy range is inexplicable.

Before presenting our LDA vibrational modes we discuss one-ball models for the vibrational modes of the polymerized C_{60} molecules and for the vibrational modes due to an fcc lattice of C_{60} molecules. These two simple models show how perturbations induced on a single ball lead to qualitatively different mixings between the IR active F_{1u} modes and the optically silent vibrational modes. As demonstrated below, the dimerized model is quite physical and describes well the primary perturbations that occur upon dimerization. Here we consider empirical perturbations on the LDA-based FC matrix of an isolated C_{60} molecule that was determined by Quong, Pederson, and Feldman [7]. Independent LDA-based calculations by ourselves, Wang, Wang, and Ho, and Antropov and coworkers [8–10] have shown that LDA reproduces the ten Raman active modes and four IR active modes to approximately 20–30 cm^{-1}. While similar accuracy for the optically silent modes is expected and is sufficient to explain the appearance of multiple peaks, it will not always correctly determine relative intensities of neighboring peaks.

Assuming a chain of polymerized C_{60} molecules, the on-ball perturbations of the C_{60} FC matrix are primarily due to diagonal changes associated with the four atoms in Fig. 1 that are at the poles of adjacent C_{60} molecules. As justified below, the fourfold coordination of the polar carbon atoms spherically alizes the diagonal block of the FC matrix, and a useful model is to replace the anisotropic diagonal blocks of these atoms by an isotropic matrix with $h_{xx} = h_{yy} = h_{zz} = (991\ cm^{-1})^2$ and $h_{xy} = 0$ for $x \neq y$. The resulting FC matrix exhibits the symmetry associated with the eight reflections (referred to as R_8 here) and has the same representations as the electronic analogs. The vibrational DOS is determined by diagonalizing the full (180×180) FC matrix presented in Fig. 3. In addition to the total DOS, we include the projection of the phonon DOS onto the IR active F_{1u} manifold.

By perturbing the diagonal blocks associated with dimers along the x, y, and z axes, we produce a FC matrix with the symmetry (T_h) of an ideal fcc lattice of C_{60} molecules. The resulting spectrum has odd and even threefold representations and six onefold representations transforming like (x, y, z), (xy, yz, zx), 1, xyz, b, b^*, $xyz \times b$, and $xyz \times b^*$, respectively [$b = xx + \exp(i2\pi/3)yy + \exp(i4\pi/3)zz$]. The b representations are degenerate since they are related by complex conjugation. Diagonalizing the full FC matrix leads to the phonon DOS that is also exhibited in Fig. 3. Comparison of the T_h and R_8 DOS shows that polymerization leads to splittings that are not observed in the T_h structure. Analysis of the $F_{1u}(4)$ peak (near 1450 cm^{-1}) shows that the

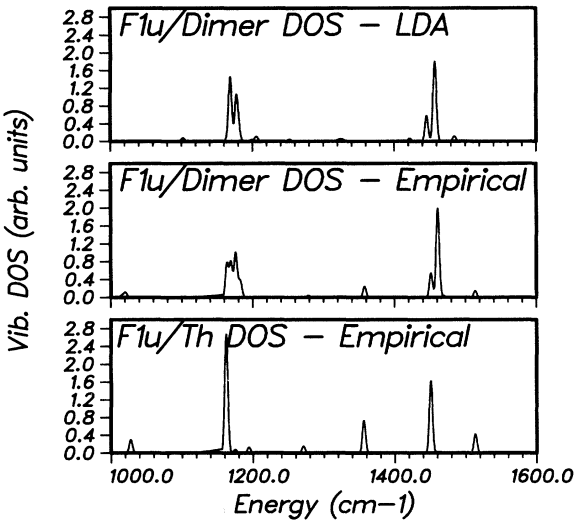

FIG. 3. Broadened F_{1u}-projected vibrational DOS obtained for one-ball model calculation with T_h and R_8 symmetries, respectively. Top panel includes the LDA projected F_{1u} vibrational DOS of the dimer.

two-peaked (R_8) structure at this energy is due to mixing between the optically inactive $G_u(6)$ level and one of the IR active $F_{1u}(4)$ levels. 80% of the F_{1u} states remain within 10 cm^{-1} of their isolated peak, and additional activation, also present in the T_h model, occurs at lower and higher energies due to mixing with the neighboring $H_u(7)$, $G_u(6)$, and $F_{2u}(4)$ levels. The twin peaks near the original $F_{1u}(4)$ line are a direct consequence of the reduced symmetry and can be understood from the following.

For both models, the phonon eigenvectors show that the only levels contributing to the spectrum in the $F_{1u}(4)$ energy range are the $F_{1u}(4)$ states and the $G_u(6)$ states. These two states are strongly coupled because they are energetically nearly degenerate and because the portions of the phonon eigenvectors that reside on the polar dimers are nearly linearly dependent. For the T_h model, the optically silent $G_u(6)$ level is split into onefold and threefold representations. The latter representation mixes with the $F_{1u}(4)$ mode leading to the emergence of two threefold peaks that can be IR active. A simple two-state analysis shows that the mixed modes are split by $[(\epsilon_1 - \epsilon_2)^2 + (\Delta/\epsilon_c)^2]^{1/2}$, where ϵ_1 and ϵ_2 are the energies of the *unperturbed* F_{1u} and G_u states, Δ is the coupling constant, and $\epsilon_c = (\epsilon_1 + \epsilon_2)/2$. The coupling constant is of order $(\frac{12}{60})(\frac{991}{2})^2$ cm^{-2} suggesting that the two peaks arise from the $F_{1u}(4)$-$G_u(6)$ splitting of approximately $\Delta/\epsilon_c = 135$ cm^{-1}. A more accurate determination is obtained by diagonalizing the full matrix leading to a splitting of 95 cm^{-1} and the appearance of a strong and weak IR active peak that are 10 and 105 cm^{-1} below the original $F_{1u}(4)$ peak.

The emergence of a double peak, with a smaller splitting, near the pure $F_{1u}(4)$ level for the polymerized R_8 model is then explained by noting that the (x, y) rows of the $F_{1u}(4)$ and $G_u(6)$ are essentially unperturbed in the R_8 model so they retain their icosahedral energies, structure, and level of IR activity (or inactivity). However, the z rows of the $G_u(6)$ and $F_{1u}(4)$ states are perturbed and lead to peaks at the same energies as in the T_h model. The double peak near the $F_{1u}(4)$ energy is a clear indication of strong coupling between the z rows of the $G_u(6)$ and $F_{1u}(4)$ representations and indicates a significant degree of symmetry lowering. The relative intensities of the two peaks at the $F_{1u}(4)$ energy is a clear indicator of the relative energy of the unperturbed $G_u(6)$ level. Our low-intensity peak at lower energy arises because our isolated-molecule LDA calculations predict a $G_u(6)$ energy lower than the $F_{1u}(4)$ energy. Since no first-principles or empirical models reproduce the Raman and IR modes to better than 20–30 cm^{-1} the relative peak positions obtained theoretically may be (and are) juxtaposed and shifted in comparison to experiment.

An additional feature of the dimer DOS is the broadening of the lower $F_{1u}(3)$ level into at least three peaks. This is also present in the slow cooled IR measurements of Mihaly *et al.* which show two strong peaks in this energy range and additional structure approximately 10 cm^{-1} higher in energy. Examination of the phonon eigenvectors in this region show that they are composed of the icosahedral $F_{2u}(4)$, $F_{1u}(3)$, and $H_u(5)$ eigenvectors. In the T_h model the $H_u(5)$ and $F_{2u}(4)$ retain much of their icosahedral identity with less than 4% of the F_{1u} admixture. Thus there is a nearly pure $F_{1u}(3)$ peak plus two very small peaks in the third panel of Fig. 3. In contrast, for the R_8 model, there are at least three distinct peaks, spread out over approximately 20 cm^{-1} that have $F_{1u}(3)$ admixtures ranging between 17% and 100%.

The dimer modes can be determined more exactly within the LDA framework by direct calculation of the dimer-induced perturbations of the FC matrix. To obtain the perturbed FC matrix elements for the 12 light colored carbon atoms in Fig. 1, we have calculated the forces associated with the hydrogenated analog of the white carbon atoms in Fig. 1 at the equilibrium geometry and for small displacements from the equilibrium geometry. This allows the determination of the FC matrix elements between coordinates on the four-membered ring and the eight backbonded carbon atoms. As above, we assume that the remaining elements of the FC matrix are identical to the elements of the isolated C_{60} molecules [7] and we project the perturbed spectrum onto the isolated F_{1u} states to show changes in IR activity. The total and projected vibrational DOS is shown in Fig. 4.

This calculation shows that the simple model discussed above contains much of the relevant physics. The diagonal FC matrix associated with a polar atom is indeed more isotropic. For an isolated C_{60} molecule the diagonal elements are $h_{xx} = (1200\ cm^{-1})^2$, $h_{yy} = (1045\ cm^{-1})^2$, and $h_{zz} = (644\ cm^{-1})^2$, whereas for the C_{60} dimer, we find $h_{xx} = (945\ cm^{-1})^2$, $h_{yy} = (1075\ cm^{-1})^2$, and $h_{zz} = (922\ cm^{-1})^2$. The perturbation of the FC matrix is reasonably well localized to the four-membered ring; the

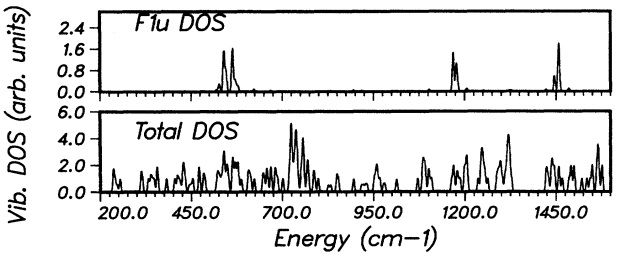

FIG. 4. The total and projected F_{1u} vibrational DOS of the C_{60} dimer as calculated from the LDA.

diagonal FC matrix elements of the eight backbonded atoms change by less than 10%.

The LDA FC matrix reproduces many of the qualitative features observed experimentally by Mihaly *et al.* and by the empirical model discussed above. The $F_{1u}(4)$ mode is split into two peaks that are separated by 10 cm^{-1}. Other peaks appear that correlate with observed IR activation at other energies. A qualitative difference between the LDA results and the empirical model appears near the $F_{1u}(3)$ energy range. Both dynamical matrices lead to five states composed of $F_{1u}(3)$, $F_{2u}(4)$, and $H_u(5)$ character which are expected to be IR active, since they are partially composed of F_{1u} symmetry. However, the LDA DOS leads to a predominantly two-peaked structure in contrast to the empirical model that yields a three-peaked structure plus a shoulder. The DOS in this region is clearly sensitive to quantitative details of the calculation. The LDA DOS more closely resembles the IR transmission data of Mihaly *et al.* [2(c)]; the additional structure at 1207 cm^{-1} observed in their measurements may be due to one or two formerly silent ungerade modes.

In summary, fullerene polymers are energetically stable and lead to a CTC distance that is significantly shorter than observed in the fcc structures. The peaks near the $F_{1u}(4)$ energy range are caused by level mixing between the axial modes of the optically silent $G_u(6)$ and $F_{1u}(4)$ manifolds; significantly larger splitting of the $F_{1u}(4)$ manifold (approximately 80 cm^{-1}) occurs when the interrepresentational couplings are artificially turned off. Because of the presence of two other optically inactive modes in the $F_{1u}(3)$ energy range, quantitative determination of the number of peaks is more complicated. Our empirical model shows the symmetry-allowed appearance of a multipeaked structure in the $F_{1u}(3)$ energy range but our LDA results suggest a two-peaked structure.

While the $[C_{60}]_2$ molecule could dimerize in other ways and forms structures with a single C-C bond between two balls our intent has been to determine the electronic, vibrational, and cohesive energies relevant to the structures proposed in Refs. [1(b)] and [5]. The one-ball models show that reasonable perturbations of the C_{60} FC matrix lead to qualitatively different F_{1u} DOS when T_h (fcc) rather than R_8 (dimer) symmetry is imposed. Since the splittings in the vibrational spectrum are primarily caused by a mixing between optically inactive and active modes, it is possible that C_{60} chains with a qualitatively *different* connectivity could lead to a qualitatively *similar* IR spectrum. In slight discord with experiment is our prediction of a normal polar C-C bond length of 1.57 Å and a slightly shorter CTC distance. The small underestimate of the CTC distance could be due to Rb-C hard-sphere repulsions, to partially screened Coulomb repulsions between C_{60} molecules, or to incomplete relaxation of our geometry. From experiment, it is known that rubidium may enhance the C_{60} CTC distance by 0.24 Å in Rb_3C_{60} [11].

We thank Professor L. Mihaly and M. C. Martin for experimental IR data prior to publication and many informative discussions and Dr. J. Q. Broughton and Dr. S. C. Erwin for helpful discussions. M. R. P. was supported in part by the ONR and C90 time from CEWES. A. A. Q. thanks the NRC and the U.S. DOE, Office of Basic Science, Materials Science Division.

Note added.—Since submission we have recalculated the LDA cohesive energy for a fully relaxed C_{60} dimer; the CTC distance is 9.1 Å and the dimer is bound by 1.2 eV [12].

[1] (a) O. Chauvet *et al.*, Phys. Rev. Lett. **72**, 2721 (1994); (b) P. W. Stephens *et al.*, Nature (London) **370**, 636 (1994).

[2] (a) M. C. Martin *et al.*, Phys. Rev. B **47**, 14 607 (1993); (b) M. C. Martin *et al.*, Phys. Rev. B **51**, 3210 (1995); (c) L. Mihaly *et al.*, in *Progress in Fullerene Research,* edited by H. Kuzmany, J. Fink, M. Mehring, and S. Roth (World Scientific, Singapore, 1994), p. 265.

[3] For cyclobutane $[C_2H_4]_2$, the reaction barrier and energy are experimentally known to be 2.7 and 0.8 eV, respectively, and are in accord with our LDA energetics of 2.3 and 1.7 eV. The reaction energy within the generalized gradient approximation is 1.04 eV for cyclobutane. For experimental energetics see W. Doering, Proc. Natl. Acad. Sci. USA **78**, 5279 (1982).

[4] (a) P. Zhou *et al.*, Chem. Phys. Lett. **211**, 337 (1993); (b) Y. Wang *et al.*, Chem. Phys. Lett. **217**, 413 (1994); (c) A. M. Rao *et al.*, Science **259**, 955 (1993).

[5] S. Pekker *et al.*, Solid State Commun. **90**, 349 (1994).

[6] M. R. Pederson and K. A. Jackson, Phys. Rev. B **41**, 7453 (1990); **43**, 7312 (1991); K. A. Jackson and M. R. Pederson, *ibid.* **42**, 3276 (1990).

[7] A. A. Quong, M. R. Pederson, and J. L. Feldman, Solid State Commun. **87**, 535 (1993).

[8] X. Q. Wang, C. Z. Wang, and K. M. Ho, Phys. Rev. B **48**, 1884 (1993).

[9] V. P. Antropov, A. I. Liechtenstien, and O. Gunnarsson, Phys. Rev. B **48**, 7651 (1993); V. P. Antropov (private communication).

[10] J. C. R. Faulhaber, D. Y. K. Ko, and P. R. Briddon, Phys. Rev. B **48**, 662 (1993).

[11] W. I. F. David *et al.*, Europhys Lett. **18**, 219–225 (1992); R. M. Fleming *et al.*, Nature (London) **352**, 787 (1991).

[12] D. V. Porezag, B. Davidson, and M. R. Pederson (unpublished).